INVESTIGATION OF THE COMPRESSION PERFORMANCE AND FAILURE MECHANISM OF PSEUDO-DUCTILE THIN-PLY HYBRID COMPOSITES

Gergely Czél[1,2], Putu Suwarta[2], Meisam Jalalvand[2], Michael R. Wisnom[2]

[1]Department of Polymer Engineering, Faculty of Mechanical Engineering, Budapest University of Technology and Economics, Műegyetem rkp. 3. H-1111 Budapest, Hungary, czel@pt.bme.hu, www.pt.bme.hu
[2]Bristol Composites Institute (ACCIS), University of Bristol, Queen's Building, BS8 1TR, Bristol, United Kingdom, putu.suwarta@bristol.ac.uk, M.Jalalvand@bristol.ac.uk, M.Wisnom@bristol.ac.uk, http://www.bristol.ac.uk/composites/

Keywords: Hybrid composite, Compression, Fragmentation, In-situ imaging

ABSTRACT

Glass/carbon hybrid specimens were designed and loaded in four point bending in order to generate stable compressive failure which allows for detailed microscopic study of the damage mechanisms. An optical measurement technique based on the displacements of five dots on the specimen edge was applied to monitor the strain of the carbon layer from the curvature of the sample. A loading frame suitable to be inserted into the vacuum chamber of a scanning electron microscope was developed. A previously tested specimen was deformed again in the loading frame and its polished edge surface was scanned while it was kept under significant deformation. This technique was successful in visualising the microscopic deformations and allowed for a deeper understanding of the damage mechanisms. Compressive fragmentation, sliding along the inclined fracture surfaces and local delaminations around the crack tips were confirmed by micrographs. An explanatory schematic was generated, highlighting the microscopic displacements of a fragment upon further loading.

1 INTRODUCTION

High performance polymer matrix composites are suitable for high-tech applications such as military and civil aerospace, spacecraft or motorsports due to their outstanding specific stiffness and strength, fatigue and corrosion resistance. However, a fundamental limitation of current fibre reinforced composites is their inherent brittleness which has hindered their spread towards many high volume applications. Failure of composites can be sudden and catastrophic, with little or no warning and usually poor residual load-carrying capacity if any. High performance composites showing progressive damage and gradual failure similar to that of ductile metals are therefore of significant interest and could extend the scope of applications towards new fields such as automotive or construction.

The authors presented favourable pseudo-ductile failure in unidirectional (UD) glass/carbon [1] and carbon/carbon [2] fibre hybrid composites in tension recently. Since pure tensile loading is not typical of real structures, characterisation of the compression behaviour of such materials is also crucial to demonstrate their suitability for a wide range of applications.

Compressive characterisation of UD composites is more demanding then tensile testing, because the specimens need to be perfectly aligned and supported against buckling. Several test fixture designs and corresponding specimen types have evolved since the early seventies. The main approaches for direct compression testing are shear-loaded specimens with short, unsupported gauge sections according to ASTM D3410 / D3410M – 03 [3] and end-loaded specimens with anti-buckling support as specified in ASTM D695 – 10 [4]. Both test setups have advantages and shortcomings, therefore combined end- and shear loading fixtures were developed in the mid-nineties. The so called Imperial College rig [5] was presented first in 1994 and then the Combined Loading Compression (CLC) fixture [6] in 1997, which was standardised as ASTM D6641 / D6641M in 2001 [7]. These are

currently the most successful fixtures both combining end- and shear load transfer to minimise stress concentrations and premature failure around the ends of the specimens. However, the combined loading technique requires expensive, time consuming precision machining of the loaded and clamped surfaces of the specimens and simple optical video-extensometers are usually difficult to apply due to the constrained space and problem of providing adequate lighting conditions. Therefore the strains are usually monitored by less simple procedures such as use of strain gauges on both sides of the specimen involving extra preparation. The failure strains determined even with these advanced techniques are still affected by stress concentrations and shear stresses around the tabs and grips. The specimens usually show the shear instability failure type typical of most UD carbon fibre composites. The ASTM D5467/D5467M-97 [8] standard recommends a relatively large sandwich beam and four point bending test setup for compressive testing. The manufacturing of this specimen type is expensive and complicated, and the failure type may not always be acceptable (e.g. the composite skin may de-bond or the core may be crushed), therefore this technique has never been widely adopted.

The points above clearly show that direct compression testing is particularly challenging due to issues with premature failure triggered by global buckling and stress concentrations at the gripping regions. Therefore a new method was proposed recently, based on four point bending of monolithic hybrid specimens (see Fig. 1) made of several glass/epoxy plies as a backfill and a thin carbon/epoxy layer which is subject to investigation [9]. Advantages of this technique include a stress-concentration free central section under constant compressive load and potential for stable failure which is essential for damage mode observations under microscope. However it has to be noted, that failure strain and stress results obtained from bending specimens are not directly comparable to those of direct compression tests. This is because the stressed volume is small and there is a stress gradient through the thickness. Both of these effects are expected to result in increased compressive failure strains and stresses which therefore cannot be used as design allowables.

The aim of this study is to understand the compressive failure behaviour and identify the damage mechanisms of glass/carbon hybrid composites from four point bending tests.

2 MATERIALS

The hybrid composite constituent materials considered for design, and applied in the four point bending tests were standard thickness E-glass/epoxy and S-glass/epoxy prepregs supplied by Hexcel, and a thin carbon/epoxy prepreg from North Thin Ply Technology (see Tables 1 and 2). The epoxy resin systems in the prepregs were the aerospace grade 913 (Hexcel) and ThinPreg 120 EPHTg- 402 (North TPT). Both resins in the designed hybrid laminates were 120°C cure epoxies, which were found to be compatible, although no details were provided by the suppliers on the chemical formulation of the resins. Good integrity of the hybrid laminates was confirmed during test procedures and no phase separation was observed on cross sectional micrographs. Basic properties of the applied fibres and prepreg systems can be found in Tables 1 and 2.

Fibre type	Manufacturer	Elastic modulus	Density	Tensile strain to failure	Tensile strength
		[GPa]	[g/cm^3]	[%]	[GPa]
Torayca M55JB	Toray	540	1.91	0.8	4.02
EC9 756 P109 E-glass	Owens Corning	72	2.56	4.5	3.5
FliteStrand S ZT S-glass	Owens Corning	88	2.45	5.5	4.8-5.1

Table 1: Fibre properties of the applied UD prepregs based on manufacturer's data determined from impregnated strands except for the S-glass where single fibre tests were performed

Prepreg type	Fibre mass per unit area	Cured ply thickness	Fibre volume fraction	Initial elastic modulus	Tensile strain to failure	Compressive strain to failure
	[g/m^2]	[µm]	[%]	[GPa] (CV [%])[a]	[abs%] (CV [rel%])	[%]
M55 carbon/epoxy	30	30.5	52	280.0[b]	0.6[c]	0.26[c]
E-glass/epoxy	192	140	54	40.0[b]	3.07[c]	-
S-glass/epoxy	190	155	51	45.7 (3.2)[10]	3.98 (1.1)[10], 3.56[c]	2.33[c]

[a]Coefficient of variation
[b]Calculated for the given fibre volume fraction
[c]Based on manufacturer's data for 60% fibre volume fraction

Table 2: Cured ply properties of the applied UD prepregs (Figures with references are measured values.)

3 EXPERIMENTAL METHODS

Four point bending tests were executed at a constant 3 mm/min crosshead speed on a computer controlled Instron 8872 type 25 kN rated universal servo-hydraulic test machine with a regularly calibrated 10 kN rated load cell. The inner and outer spans were set to 20 and 60 mm respectively (see Fig. 1). The asymmetric UD interlayer hybrid specimens were designed to be reasonably thick (up to 3 mm) to generate significant compressive strain near the surfaces at small deflections in order to minimize the geometric non-linearity of the load-deflection response. The carbon layer was introduced in the laminate close to one surface (see Table 3 for lay-up sequence) to maximise its strain while protecting it from contact forces on the specimen surface at load insertion points by a single S-glass/epoxy ply. Rubber pads (see Fig. 2) were placed under the inner loading noses to prevent premature local compressive failure of the specimen surface due to excessive concentrated contact forces. A schematic of the test setup and the specimen design is shown in Fig. 1. Table 3 shows the lay-up sequence and the geometry of the specimens.

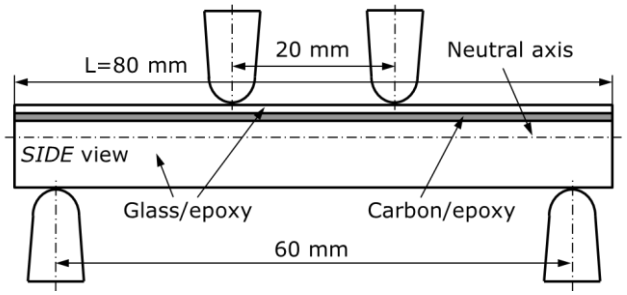

Figure 1: Schematic of the four point bending test setup with an asymmetric interlayer hybrid specimen [9].

Specimen type designation	Lay-up sequence	No. of tested specimens	Nominal thickness	Width	Support span	Inner span
			[mm]	[mm]	[mm]	[mm]
Asymmetric M55	$[SG_2/EG_{13}/SG_2/M55_2/SG_1]$	5	2.71	8	60	20

Table 3: Four point bending specimen structure and geometry (Designation: SG- S-glass, EG- E-glass)

The strain in the carbon layer was evaluated from the curvature of the specimen which was determined optically from the displacements of five dots at the edge of the specimen. The neutral axis was calculated from a laminated plate analysis assuming linear strain variation through the thickness. Load-strain diagrams were plotted and carbon layer damage and failure was detected based on the change of the slope or load drops. This novel strain evaluation technique is discussed in detail in [9].

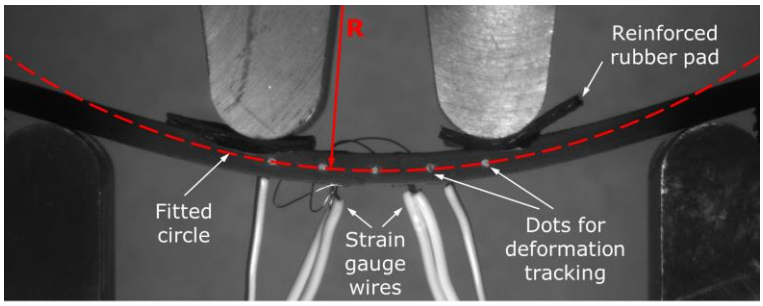

Figure 2: Annotated video frame showing the principle of optical strain measurement [9]

The damage in the specimens was analysed with a Jeol JSM 6380 LA type scanning electron microscope (SEM) while the specimen was kept under constant deformation. A loading frame was designed and manufactured with electric wire cutting from a 10 mm thick ground steel plate for this purpose as shown in Fig. 3. The contact regions have 5 mm radii, and both spans are kept the same as that of the fixture mounted on the test machine. The desired deformation was applied with an Allen key while the whole frame with the specimen had to be kept flat e.g. on a board or desk. The approximate deflection was measured with a caliper from the change of the gap size between the loading nose and the frame. This way the cracks were forced open which assured easier detection and investigation of possible microscopic deformations indicating the type of the active damage and failure mechanisms.

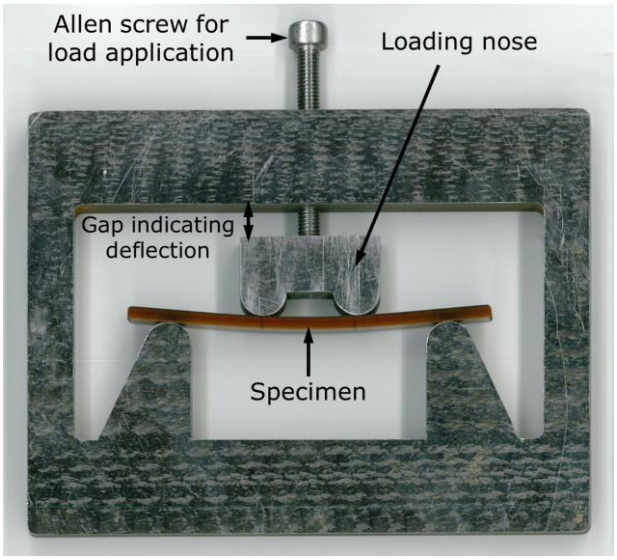

Figure 3: Four point bending frame for microscopy under deformation

4 RESULTS AND DISCUSSION

A previous study revealed that thin, high modulus carbon reinforced epoxy layers fail progressively in glass/carbon hybrid specimens as a smooth degradation of the specimen stiffness was detected in the load-strain diagrams with no load-drop. Fig. 4 shows a typical force-compressive strain diagram for a M55 carbon/epoxy layer with fitted lines highlighting the change in the slope of the curve. With

this particular fibre type and specimen configuration a 15.3% decrease of slope was detected (average of 5 specimens). This is close to the 20% contribution of the carbon layer to the full bending stiffness of the specimens calculated with the classical laminate theory (CLT). A key question of this study is what microscopic damage mechanisms allow for such reduction in the stiffness contribution of the carbon layer.

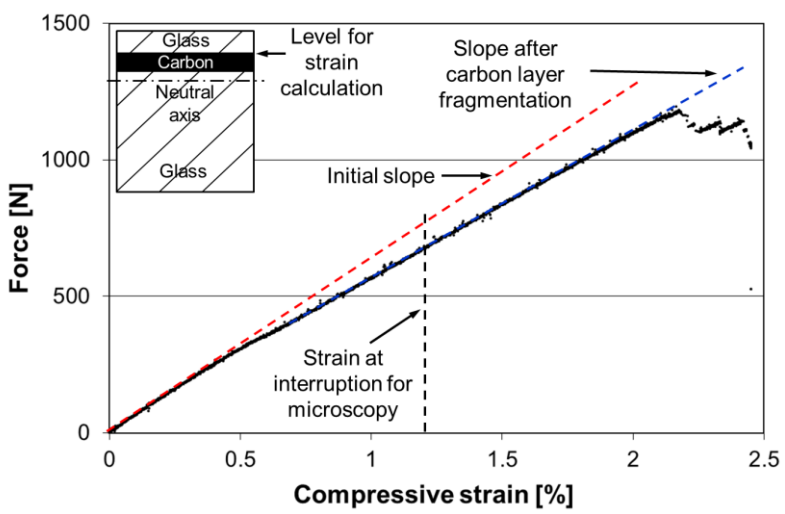

Figure 4: Typical force-compressive strain diagram of an interlayer hybrid specimen containing an M55 carbon fibre/epoxy layer

Previously a striped pattern was visible under the surface of the specimens (see Fig. 5) through the transparent glass/epoxy top layer, which was attributed to progressive fracturing (i.e. fragmentation) of the carbon layer and stable, localised delamination around the carbon layer fractures. This is an uncommon damage mode which has not been reported widely in the literature for compression tests, therefore it deserves further investigation.

Figure 5: Striped pattern in top view indicating periodic damage inside a hybrid specimen after an interrupted four point bending test [9]

In order to confirm the existence of fragmentation and local delamination, SEM images were taken first from a larger section of the edge of a specimen which had been previously loaded until 700 N force, which corresponds to 1.2% maximum strain in the carbon layer. This load level was selected as it is substantially above the knee point on Fig. 4 which was determined to be at 0.46% strain and 295 N bending force (average of 5 specimens). The overall micrograph of Fig. 6 was generated while applying similar deflection to the same specimen with the developed loading frame as that applied previously in the test machine. Smaller regions of the specimen surface were scanned with high magnification and then the acquired mosaic images were stitched together in Image J software. The micrograph of Fig. 6 confirms that the carbon layer was fragmented in compression as several fractures were detected along an approximately 4 mm long section.

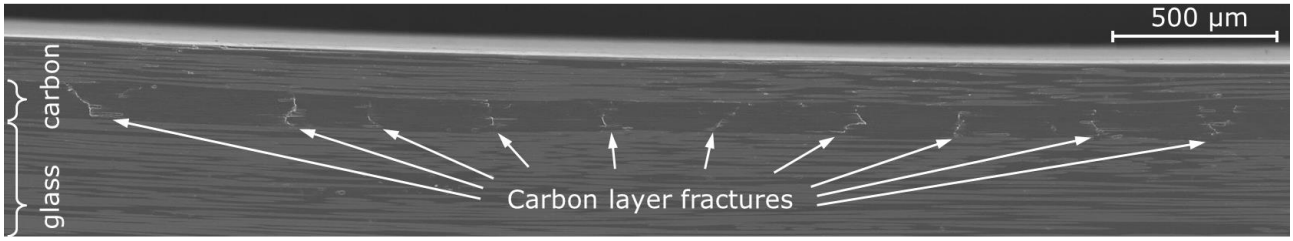

Figure 6: Carbon layer fractures on an edge view scanning electron micrograph

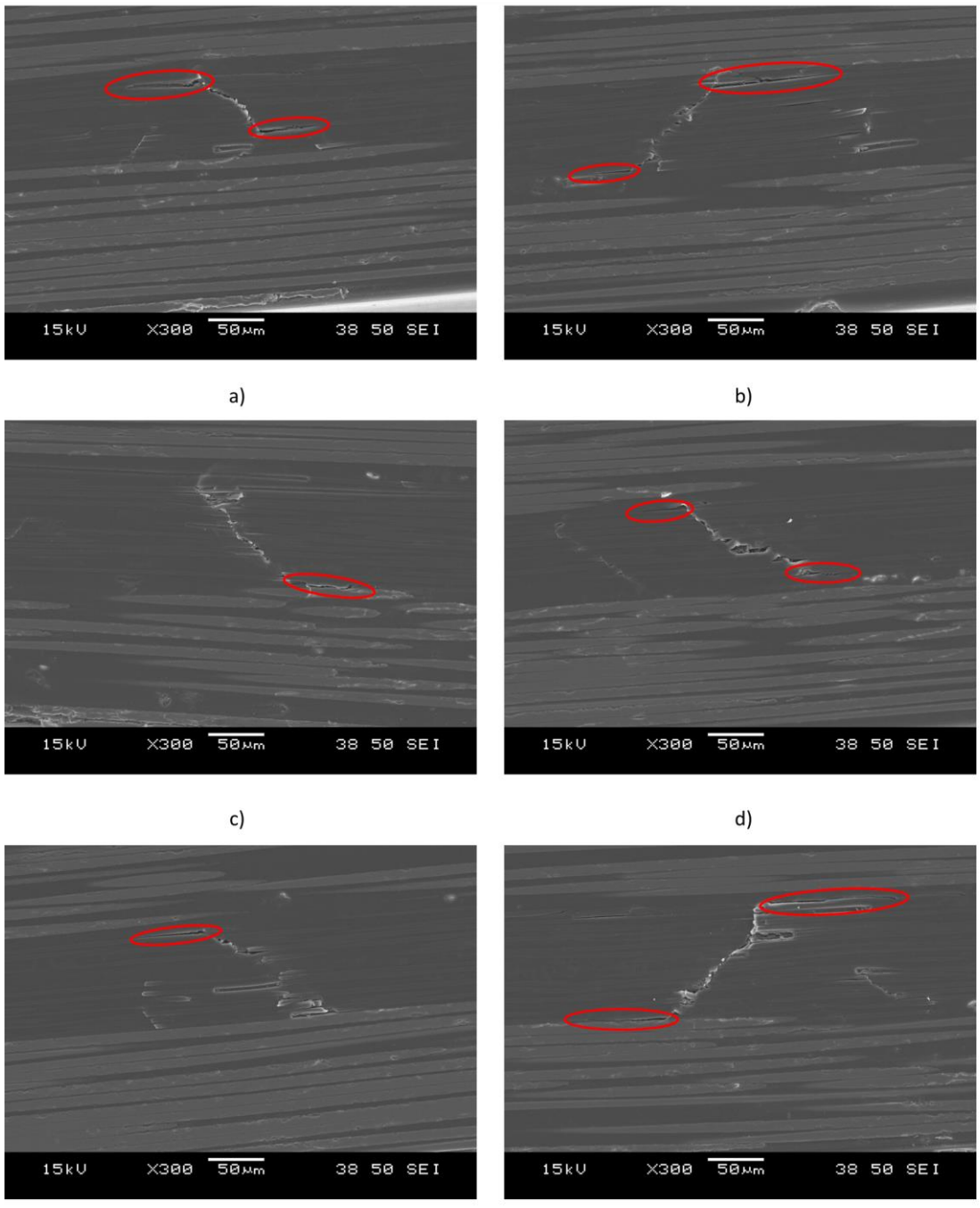

Figure 7: Scanning electron microscope close-up views of different carbon layer cracks under approx. -1.2% strain. Red ovals highlight local delaminations.

The close-up images of Fig. 7 allow for detailed analysis of the fracture morphology. The approx. 45° average angle of the carbon layer cracks suggest that translaminar shear fractures were developed. These shear cracks did not lead to instability (no kink bands detected) but appeared in a stable, progressive manner due to the support of the neighbouring glass plies. No sign of extensive fibre crushing (i.e. voids and debris) was noticed around the sharp cracks which showed up to 5 μm (around 1 fibre diameter) sliding displacement at the given 1.2% compressive strain. It is also confirmed, that local opening mode delaminations took place at the intersections of the inclined fracture lines with the layer interfaces and openings in a similar (few μm) range were detected (see highlighted regions of Fig. 7). The low transverse vs. longitudinal stiffness ratio and the low through-thickness interlaminar vs. longitudinal strength promoted the development of these interlaminar cracks. Since more severe damage is indicated by the width of the light bands on Fig. 5, the actual extent of interfacial damage accumulated in the specimen is probably larger than the detectable delaminated regions on the cross-sectional micrographs of Fig. 7. This is because preliminary damage (e.g. irreversible matrix deformation) is likely not to be visible from the edge, but may cause a change in appearance in the top view. The damage features observed on Fig. 7 suggest that after several fractures took place, the fragments were pushed further against each other and they were still carrying and transferring some compressive load across the fracture surfaces via contact forces. Upon further deformation, the fragments were sliding further along the fracture surfaces and initiated opening delaminations locally at the crack tips, where the layer interfaces were in tension. These mechanisms are estimated to be capable of accommodating most of the additional strain in the carbon layer after fragmentation. Fig. 8 shows the anticipated microscopic deformations and damage modes schematically based on the observations made from the micrographs.

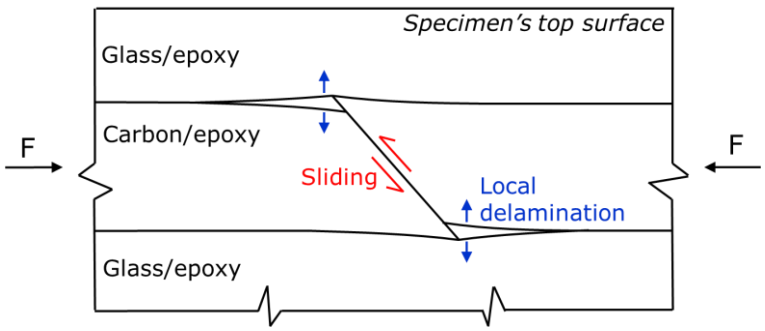

Figure 8: Schematic of the micro-deformations around a carbon layer fracture

5 CONCLUSIONS

Microscopic deformations and damage mechanisms of a carbon/epoxy layer under compression were revealed using a purpose-designed four point bending frame. Following an initial mechanical test, the specimen was reloaded in a flat fixture whilst it was kept in the vacuum chamber of a scanning electron microscope.

Progressive fragmentation of the carbon layer in a glass/carbon hybrid specimen was confirmed by stitched scanning electron micrographs revealing several carbon layer fractures within a relatively long section of the specimen edge under significant compressive strain.

Sliding of the fragments along the inclined fracture surfaces and local delaminations at the crack tips were revealed by close-up micrographs.

The anticipated micro-mechanisms based on the micrographs were understood and visualised on a longitudinal edge-view schematic of the relevant part of the four point bending specimen.

ACKNOWLEDGEMENTS

This work was funded under the UK Engineering and Physical Sciences Research Council Programme Grant EP/I02946X/1 on High Performance Ductile Composite Technology in collaboration with Imperial College London. Gergely Czél acknowledges the Hungarian Academy of Sciences for funding through the János Bolyai scholarship and the Hungarian National Research, Development and Innovation Office - NKFIH for funding through grants ref. OTKA K 116070 and OTKA PD 121121. The authors acknowledge Hexcel and North TPT for supplying materials for this research. All data required for reproducibility are provided within the paper.

REFERENCES

[1] G. Czél, M. Jalalvand, M.R. Wisnom, Design and characterisation of advanced pseudo-ductile unidirectional thin-ply carbon/epoxy-glass/epoxy hybrid composites, Composite Structures, **143**, 2016, pp. 228-238 (doi: https://doi.org/10.1016/j.compstruct.2016.02.010)

[2] G. Czél, M. Jalalvand, M.R. Wisnom, T. Czigány, Design and characterisation of high performance, pseudo-ductile all-carbon/epoxy unidirectional hybrid composites, Composites Part B: Engineering, **111**, 2017, pp. 348-356 (doi: http://dx.doi.org/10.1016/j.compositesb.2016.11.049)

[3] ASTM D3410 / D3410M – 03 (2008) Standard Test Method for Compressive Properties of Polymer Matrix Composite Materials with Unsupported Gage Section by Shear Loading

[4] ASTM D695 – 10 Standard Test Method for Compressive Properties of Rigid Plastics

[5] J.G. Haberle, F.L. Matthews, An improved technique for compression testing of unidirectional fibre-reinforced plastics; development and results, Composites, **25**, 1994, pp. 358-371. (doi: https://doi.org/10.1016/S0010-4361(94)80006-5)

[6] D.F. Adams, J.S. Welsh, The Wyoming Combined Loading Compression (CLC) Test Method, Journal of Composites Technology and Research, **19**, 1997, 123-133.

[7] ASTM D6641 / D6641M – 14 Standard Test Method for Compressive Properties of Polymer Matrix Composite Materials Using a Combined Loading Compression (CLC) Test Fixture

[8] ASTM D5467/D5467M-97 Standard Test Method for Compressive Properties of Unidirectional Polymer Matrix Composite Materials Using a Sandwich Beam

[9] G. Czél, M. Jalalvand, M.R. Wisnom, Hybrid specimens eliminating stress concentrations in tensile and compressive testing of unidirectional composites, Composites Part A: Applied Science and Manufacturing, **91**, 2016, pp. 436-447 (doi: http://dx.doi.org/10.1016/j.compositesa.2016.07.021)

[10] Czél G, Jalalvand M, Wisnom MR. Demonstration of pseudo-ductility in unidirectional hybrid composites made of discontinuous carbon/epoxy and continuous glass/epoxy plies. Composites Part A: Applied Science and Manufacturing, **72**, 2015, pp. 75-84. (doi: http://dx.doi.org/10.1016/j.compositesa.2015.01.019)